I&EC research
Industrial & Engineering Chemistry Research

Article

Cite This: Ind. Eng. Chem. Res. 2018, 57, 4640−4650

pubs.acs.org/IECR

Simultaneous Thermal Cross-Linking and Decomposition of Side Groups to Mitigate Physical Aging in Poly(oxyindole biphenylylene) Gas Separation Membranes

Hugo Hernández-Martínez,[†] F. Alberto Ruiz-Treviño,[*,†] J. Ortiz-Espinoza,[†] Manuel J. Aguilar-Vega,[‡] Mikhail G. Zolotukhin,[§] Raymundo Marcial-Hernandez,[§] and Lilian I. Olvera[∥]

[†]Departamento de Ingeniería y Ciencias Químicas, Universidad Iberoamericana, Prol. Paseo de la Reforma No. 880, Lomas de Santa Fe, Ciudad de México 01219, México

[‡]Unidad de Materiales, Centro de Investigación Científica de Yucatán, A. C., Calle 43 por 32 y 34 No. 130, Chuburná de Hidalgo, 97205, Mérida, Yucatán, México

[§]Instituto de Investigación en Materiales, Universidad Nacional Autónoma de México, Apartado Postal 70-360, CU, Coyoacán, Ciudad de México 04510, México

[∥]CONACYT-Centro de Investigación y Desarrollo Tecnológico en Electroquímica, Parque Industrial Querétaro, Sanfandila s/n, Pedro Escobedo, 76703 Querétaro, México

ABSTRACT: Physical aging in amorphous polymers causes a decrease in specific volume and thus in the gas transport properties of their membranes. In this work, the effect of simultaneous thermal decomposition of a thermolabile *tert*-butyl carbonate group, BOC, and cross-linking by a propargyl group ($-CH_2-C\equiv CH$) on the gas selectivity−permeability properties of the resulting membranes is studied to learn how membranes with mitigated variations in the gas permeability coefficients with aging time may be produced. The model copolymer is a poly(oxyindole biphenylylene) that bears BOC and propargyl groups, $[(PN\text{-}BOC)_x\text{-}(PN\text{-}Pr)_y]_n$. Systematic studies on the structure/processing/property relationship assessed by TGA, DSC, and permeation measurement using pure gases reveal that a single thermal treatment for 1 h at 240 °C on a neat copolymer membrane, 12−20 μm thickness, is enough to produce chemically robust membranes (insoluble in NMP and DMSO) and that are physically more resistant to aging since the permeability reduction rate approaches zero. The cross-linked membranes possess lower gas permeability coefficients with higher ideal selectivity with respect to the corresponding neat copolymer membranes, i.e., the $P(H_2)$ decreases from 60 to 42 Barrers but H_2/CH_4 selectivity increases by a factor of 2 (21 to 40), and in general the selectivity−permeability properties for the gas pairs H_2/CH_4, O_2/N_2, and CO_2/CH_4 do not present drastic variations with aging time at least from 72 to 2000 h.

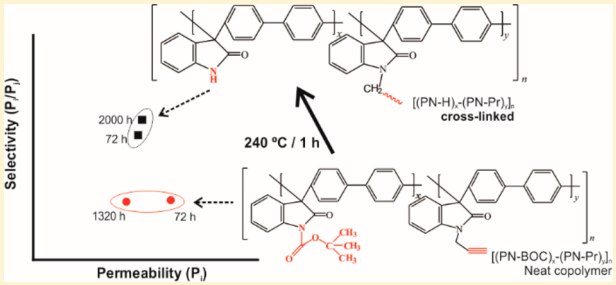

1. INTRODUCTION

Polymer membranes as gas separation means are becoming competitive basically because they are both economically attractive and environmentally friendly.[1] As compared to other gas separation processes, polymer membranes present important advantages, i.e., simple operation and compact size, among others.[2,3] Even though hundreds of polymers have been synthesized to evaluate their potential application as a membrane, just a few of them have found an application in the real field. The requirements to determine if a polymer membrane is suitable for real applications must consider several characteristics such as (1) an attractive selectivity-permeability combination, (2) an ability to be processed or fabricated as a hollow-fiber or sheet film, and (3) chemical and physical resistance to support the aggressive environments typically found in industrial applications, among other important aspects. Thus, the research and development of polymer membrane technologies, to decide if a polymer is or is not competitive as compared to commercial membranes, involves great challenges.

Among the different types of materials that have been studied for gas separation by membranes are organic polymers; cross-linked polymers; microporous organic polymers, MPOs; mixed matrix membranes, MMMs; carbon molecular sieve membranes, CMS; and inorganic membranes such as zeolites.[4−8] Specifically, a major drawback that amorphous polymers face is physical aging, which causes instability in their gas permeability coefficients with time, and this instability is a direct consequence of polymer free volume changes that result from the displacement of the nonequilibrium specific volume in the glassy state toward the specific volume that corresponds to the

Received: February 2, 2018
Revised: March 16, 2018
Accepted: March 17, 2018
Published: March 21, 2018

DOI: 10.1021/acs.iecr.8b00529
Ind. Eng. Chem. Res. 2018, 57, 4640−4650

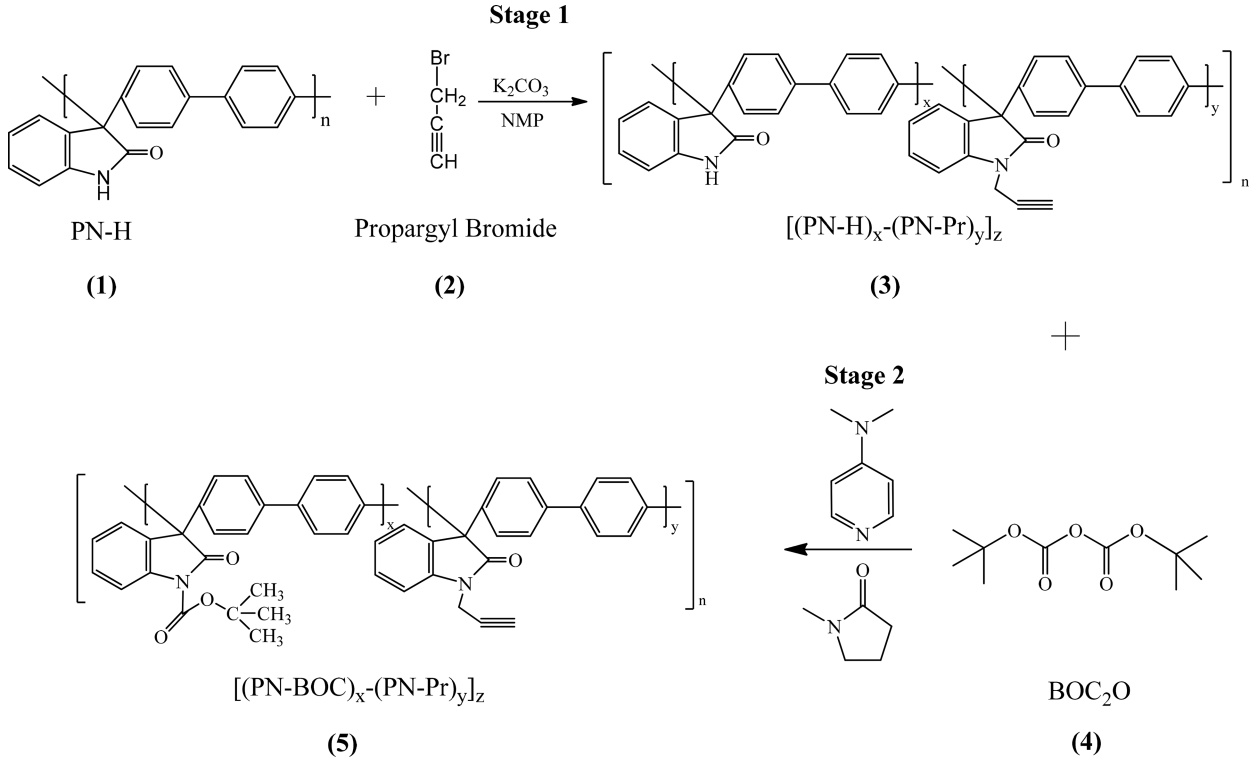

Figure 1. Chemical reaction scheme to synthesize at room temperature a pure $[PN\text{-}BOC]_x\text{-}[PN\text{-}Pr]_y$ copolymer made up of a thermolabile BOC group and an unsaturated propargyl group.

equilibrium crystalline state.[9−12] This phenomenon has been followed by different experimental techniques to understand, predict, and/or avoid it as much as possible.[9,10] Some of the polymers that have been studied in terms of the effect of aging time on permeability reduction rate and/or densification rate are polycarbonates,[13] polysulfones,[14−16] polyimides based on 6FDA,[17−20] and perfluoropolymers,[12,21] among others. Important variables that affect directly the densification or permeability reduction rate are previous processing history,[14] membrane thickness,[15,18] post-thermal treatment,[20] and type of solvent used for membrane casting.[12] Kim et al. studied the effect of aging time in thin films (300 nm) on the permeability reduction rate of non-cross-linked and cross-linked polyimides based on 6FDA.[22,23] Their results show that the cross-linked membranes possess lower gas permeability coefficients with practically the same permeability reduction rate as the corresponding non-cross-linked polyimide. Thus, at first sight it should be concluded that cross-linking is not the best alternative to mitigating the aging time effect on gas transport properties. Nevertheless, it would be instructive to learn if Kim et al.'s observation could or could not be generalized for another type of polymers since it is well-recognized that cross-linking is a useful route to reducing to some extent physical aging, on one hand, and also CO_2 plasticization, on the other hand, as it has been proved in the current literature.[22,23]

In relation to cross-linking, the current literature suggests that the unsaturated groups found in a propargyl moiety favor the cross-linking of the polymer repeating units to get useful materials for diverse applications, i.e., proton exchange membranes,[24,25] thermoplastic liquid crystalline polymers, TLCPs,[26] microporous organic polymers for CO_2 capture and H_2 storage, CMPs,[27] phenolic resins,[28−31] thermostable polymers for electric applications,[32] cross-linked polypeptoides as an alternative route to natural and synthetic polypeptides,[33] and ionic conducting membranes for gas separation.[34] In parallel, research efforts have also been focused on the evaluation of the selectivity−permeability properties of the so termed thermally rearranged polymer membranes, which possess an outstanding performance due to the formation of microcavities and fractional free volume redistribution upon a change in chemical structure promoted by thermal treatment.[35−38] Alternative modifications to produce microcavities in polymers are the incorporation of two to four *tert*-butyl carbonate groups, BOC,[39] and/or covalent attachment of *β*-cyclodextrin in polyimides[40] with the goal that upon removal under an appropriate thermal treatment, the decomposition of such thermolabile groups may form the required microcavities, leading to membranes with outstanding performance in selectivity−permeability.

Similarly, Sanchez-Garcia et al. have proposed an alternative route to produce thermally treated membranes that overcome the typical trade-off found in amorphous polymers. In their study, a single BOC moiety is incorporated as a lateral group in a poly(oxyindole biphenylylene) membrane, which once thermally decomposed at 150 °C for 1 h leads to membranes with superior selectivity−permeability properties compared to the corresponding nonthermally treated membranes.[41] Thus, as a continuation of the BOC thermally treated mentioned research, it would be instructive to learn if the simultaneous thermal decomposition of a single BOC moiety and the cross-linking with an unsaturated propargyl group may lead to robust membranes in terms of their chemical stability (insoluble to aggressive solvents) and physical stability as determined by the mitigation of the permeability reduction rate due to aging.

DOI: 10.1021/acs.iecr.8b00529
Ind. Eng. Chem. Res. 2018, 57, 4640−4650

2. EXPERIMENTAL SECTION

2.1. Materials and Polymer Synthesis. *Materials.* All starting materials were obtained from Aldrich Chemical. Di-*tert*-butyl dicarbonate (BOC), 4-dimethylaminopyridine, and propargyl bromide were used as received. N-methyl-2-pyrrolidinone (NMP) and dimethyl sulfoxide (DMSO) were distilled before use.

Polymer Synthesis. Figure 1 shows the chemical reaction route to synthesize a poly(oxyindole biphenylylene) that bears an unsaturated propargyl group ($-CH_2-C\equiv CH$) and a thermolabile BOC group (**5**). The synthesis is based on a chemical modification of a previously synthesized polymer that possesses a hydrogen atom, PN-H (**1**),[42,43] and implies two stages. In stage 1 PN-H (**1**) reacts with propargyl bromide (**2**) to obtain a partially substituted copolymer $[(\text{PN-H})_x\text{-}(\text{PN-Pr})_y]_n$ (**3**). In stage 2, copolymer **3** reacts with BOC_2O (**4**) to get $[(\text{PN-BOC})_x\text{-}(\text{PN-Pr})_y]_n$ (**5**). A typical synthesis is as follows: In a single-necked flask equipped with a magnetic stirrer, fibrous PN-H (0.5 g, 1.76 mmol) is dissolved with NMP (3 mL). Once dissolution is reached, known amounts of K_2CO_3 (0.2195 g, 1.58 mmol) and propargyl bromide (0.126 mL, 1.58 mmol) are added, and the mixture is reacted, at room temperature, for 24 h. In a second stage, a known amount of BOC_2O (0.3852 g, 1.76 mmol) and a previously prepared solution of 4-dimethylaminopyridine (0.2156 g, 1.76 mmol) in NMP (2 mL) are incorporated into the mixture, and the reaction is allowed to proceed, at room temperature, for an additional 24 h. Afterward, the high-viscosity polymer mixture is precipitated in methanol. The polymer (white fibers) is then Soxhlet extracted with methanol/acetone solutions until the complete removal of NMP. The synthesis scheme shown in Figure 1 is an alternative route to a classical reaction that involves a copolymerization with three monomers, a monomer bearing BOC, a monomer bearing propargyl, and both polymerized with a biphenylylene monomer.

2.2. Membrane Formation and Thermal Treatments. Polymer dense films were solution-cast onto a horizontal surface of cellophane using chloroform solutions containing 3 wt % of polymer. Cast films were dried at room temperature overnight, and then they were removed from the cellophane to be further vacuum-dried for an additional 24 h at 80 °C to remove residual chloroform. The thicknesses of neat copolymer membranes were between 12 and 20 μm. To produce polymeric membranes with chemical structural changes, neat copolymer membranes based on copolymer **5** were thermally treated, under a vacuum (~1 mmHg), for 1 h at three different constant temperatures, 150, 200, and 240 °C. To standardize the processing treatment applied to all membranes, the desired treatment temperature was first set in a Yamato ADP-21 vacuum oven. Once the desired temperature under a vacuum was reached and after it remained equilibrated for 20 min, every membrane was introduced to the vacuum oven for 1 h. After this time, the membrane was removed from the vacuum oven and allowed to cool down until it reached room temperature.

2.3. Polymer Membrane Characterization. Proton nuclear magnetic resonance, ^{1}H NMR, was used to determine the chemical structure and composition of the $[(\text{PN-BOC})_x\text{-}(\text{PN-Pr})_y]_n$ neat copolymer using a Bruker Avance Spectrometer. Thermogravimetric analysis, TGA (TA Instruments Q50), and differential scanning calorimetry, DSC (TA Instruments Q20), were used to determine the temperatures where the thermolabile BOC decomposes and the propargyl group reacts to cross-link the polymer chains of the repeating units and to determine the glass transition and the thermal decomposition temperatures for both the neat copolymer membrane and the thermally modified membranes. For TGA, a 10 °C/min ramp under a nitrogen flow (50 mL/min) was used from room temperature to 800 °C. The same TGA was also used to follow the thermolabile BOC isothermal kinetics decomposition evaluated at different temperatures. DSC analyses were performed at a 10 °C/min ramp under a nitrogen flow (50 mL/min) from 25 to 550 °C. Polymer densities of dried films were determined at 30 °C in a density gradient column using well-degassed $ZnCl_2$ aqueous solutions, and then the densities were used to estimate the Fractional Free Volume, FFV. Wide-angle X-ray diffraction (WAXD) scans were made for neat and thermally treated copolymers using a Xeuss Xenocs X-ray diffractometer at a Cu Kα wavelength of 1.54 Å. A corresponding d spacing, as an indicator of the average chain spacing, was calculated from the diffraction peaks maxima using the well-known Bragg equation, $n\lambda = 2d \sin\theta$. To determine the gel content as a measurement of the extent of cross-linking, GC, an initial amount, M_0, of a thermally treated membrane was immersed in NMP and DMSO for 48 h in order to reach thermodynamic equilibrium. Afterward, the swollen polymer gel was removed from the solutions and dried under a vacuum at 190 °C for at least 48 h, time where a constant weight, M_c, was reached. For this work, the GC reported, GC [%] = $(M_c/M_0)100$, corresponds to the fraction or percentage of a membrane that was insoluble in NMP and DMSO; thus, it is the fraction of cross-linked membrane. Permeability coefficients, $P(i)$, for ultrahigh purity gases H_2, O_2, N_2, CH_4, and CO_2 were measured, at 35 °C and 2 bar, in all membranes after 72 h of thermal treatment. The $P(i)$ was measured in a variable pressure/constant volume permeation cell following a well-established procedure reported elsewhere.[44] The change in gas permeability coefficients with aging time was followed for at least 2000 h in order to estimate the change in gas permeability with time, $\Delta P(i)/\Delta t$, where $\Delta P(i)$ is defined as the difference between the permeability coefficient determined at time t, $P_t(i)$, minus the permeability coefficient determined at time zero, $P_0(i)$, the time when the first measurement was made (72 h after thermal treatment). For this work, the aging rate, $[-\partial \log P/\partial \log t]$, was also determined, as it is typically defined elsewhere.[12,16] It is important to mention that all membranes were kept under a high vacuum (10^{-3} Torr) during the whole period of aging time study. The ideal selectivity between two gases is defined as the ratio of the pure gas permeability coefficients, $P(i)/P(j)$. The measurements for each gas were determined two times with an error less than 4%.

3. RESULTS AND DISCUSSION

3.1. Polymer Synthesis. An advantage that presents the poly(oxyindole biphenylylene) based on isatine, the so-called PN-H (**1**), is that it can be polymerized at room temperature and with several monomers to produce a great variety of polymer structures. Even more, its chemical structure can be easily modified by simple polymerization schemes as demonstrated by the chemical reactions depicted in Figure 1 where polymer **1** is reacted with reactant **2** to produce polymer **3**, and then polymer **3** is reacted with reactant **4** to produce polymer **5**. In fact, polymer **5** forms transparent and flexible films with appropriate mechanical properties to support the high pressures used to determine gas permeability coefficients (2 bar). Figure 2 is a characteristic ^{1}H NMR spectrum obtained

DOI: 10.1021/acs.iecr.8b00529
Ind. Eng. Chem. Res. 2018, 57, 4640−4650

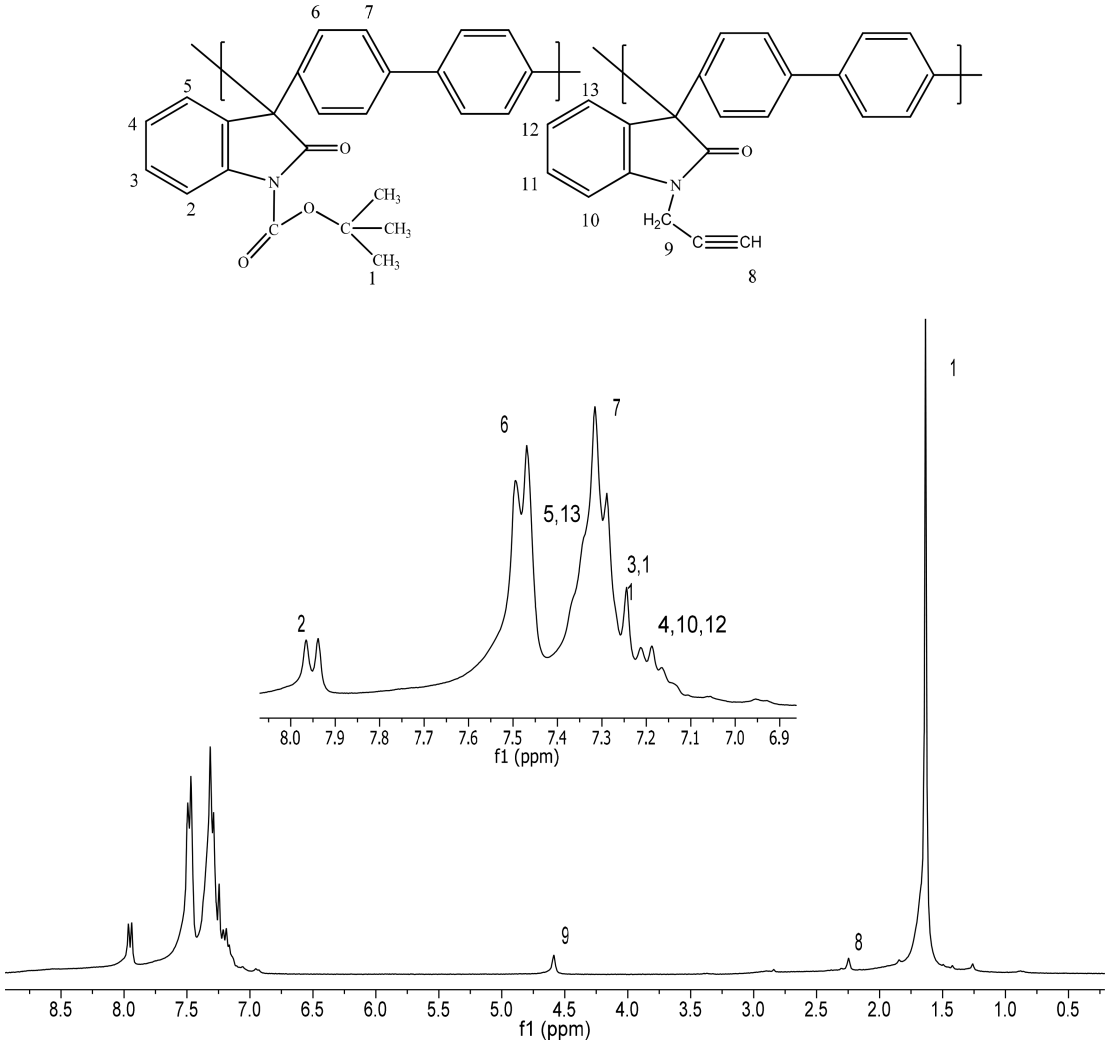

Figure 2. ^{1}H NMR spectrum for the as-synthesized copolymer $[(\text{PN-BOC})_x\text{-}(\text{PN-Pr})_y]_n$ (solution in $CDCl_3$).

for polymer **5**. The spectrum shows a singlet at 1.7 ppm that corresponds to protons of the *tert*-butyl group; the doublets at 7.3 and 7.5 ppm correspond to biphenyl protons. Signals at 2.3 and 4.5 ppm are representative of propargyl protons. The remaining signals correspond to the rest of the protons that make up the polymeric repeating unit. The ^{1}H NMR analysis confirms the chemical structure of the copolymer and also its composition. Integration carried out in the representative 4.5 ppm peak of the CH_2 group of propargyl and the representative 1.7 ppm peak of the $3(CH_3)$ groups of BOC results in a 5:1 BOC/propargyl ratio. Thus, the $[(\text{PN-BOC})_x\text{-}(\text{PN-Pr})_y]_n$ neat copolymer is made up of an approximately 83 wt % $(\text{PN-BOC})_x$ and 17 wt % $(\text{PN-Pr})_y$ block that bears a cross-linkable propargyl group.

3.2. Membrane Formation and Thermal Treatments.

Figure 3 shows TGA analysis for a recently vacuum-dried, at 80 °C for 24 h, $[(\text{PN-BOC})_x\text{-}(\text{PN-Pr})_y]_n$ membrane (curve 1), and also for membranes thermally treated, under a vacuum, for 1 h at 150 °C (curve 2), 200 °C (curve 3), and 240 °C (curve 4). The TGA analysis (curve 1) performed on the vacuum-dried neat copolymer first of all confirms that it is solvent free since no weight loss is detected below 150 °C. Moreover, the thermogram clearly presents three well-defined zones that are characterized by the following: (1) a weight loss between 150 and 200 °C, (2) a range of temperatures, from 200 to 500 °C,

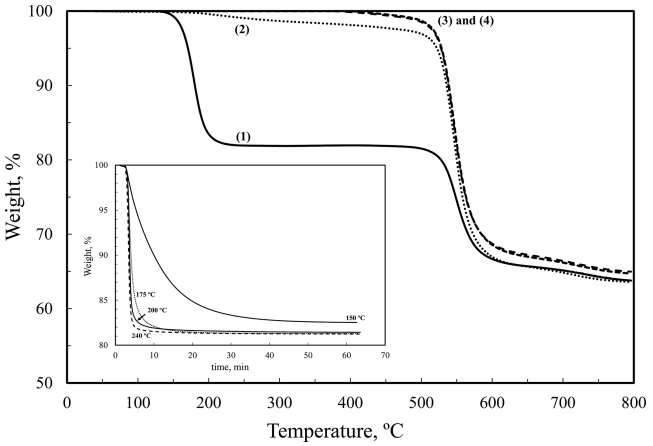

Figure 3. TGA analysis, at 10 °C/min under N_2, carried on $[(\text{PN-BOC})_x\text{-}(\text{PN-Pr})_y]_n$ neat copolymers vacuum-dried at 80 °C/24 h (1) and copolymers vacuum-thermally treated for 1 h at 150 °C (2), 200 °C (3), and 240 °C (4). Inset shows isothermal kinetics studies, at different temperatures, performed on a neat copolymer.

where there is no weight loss, and (3) a weight loss detected at temperatures higher than 500 °C. The first weight loss, approximately 18.6 wt %, corresponds to BOC thermal

DOI: 10.1021/acs.iecr.8b00529
Ind. Eng. Chem. Res. 2018, 57, 4640−4650

decomposition,[41] and this value correlates with the theoretical 21 wt % BOC in the copolymer $[(\text{PN-BOC})_x\text{-}(\text{PN-Pr})_y]_n$ (5:1 ratio from ^{1}H NMR Figure 2). The second zone where no weight is lost (from 200 to 500 °C) shows a useful temperature range to cross-link the polymer repeating units containing the propargyl group with practically no weight being lost due to cross-linking. Finally, the weight loss above 500 °C corresponds to the thermal decomposition of the copolymer main backbone chain. TGA results for the copolymers thermally treated for 1 h at different temperatures (curves 2−4) bring information with respect to the qualitative chemical changes that are occurring in the copolymer repeating units. For the copolymer treated at 150 °C, the 1−2 wt % weight loss, between 150 and 200 °C, corresponds to some BOC still present in the copolymer, and this observation is reconfirmed by the 150 °C isothermal kinetics result that has been inserted in the same Figure 3. Since there is still 1 to 2 wt % BOC, a probable chemical structure for this 150 °C treated copolymer could be that of a polymer made up of three blocks $[(\text{PN-H})_x\text{-}(\text{PN-BOC})_y\text{-}(\text{PN-Pr})_z]_n$ because, according to Sanchez-Garcia et al., the thermal decomposition of BOC in a PN-BOC leads to a PN-H polymer,[41] the starting material that is being used as a model in this study. For the copolymers thermally treated at 200 °C (curve 3), the thermogram confirms that all BOC has been decomposed, meaning that the initial $[(\textbf{PN-BOC})_x\text{-}(\text{PN-Pr})_y]_n$ copolymer has been totally converted to $[(\textbf{PN-H})_x\text{-}(\text{PN-Pr})_y]_n$. The 200 °C isothermal kinetics study (inserted in Figure 3) does really confirm that the weight loss is 18.5−19 wt %, an amount that corresponds to the BOC originally incorporated into the nonthermally treated copolymer. For the copolymer thermally treated at 240 °C, the thermogram (curve 4) and the 240 °C isothermal kinetics study (inserted in Figure 3) once again confirm that the maximum weight loss is the amount that corresponds to the block containing the BOC moiety $(\text{PN-BOC})_x$. At 240 °C, it will be expected to cross-link the copolymer repeating units containing the propargyl moiety $(\text{PN-Pr})_y$ as discussed in the following paragraphs.

Figure 4 shows DSC analysis for neat copolymer (curve 1) and for copolymers thermally treated for 1 h at 150 °C (curve 2), 200 °C (curve 3), and 240 °C (curve 4). A careful observation in each DSC shows that these copolymers do not have a glass transition temperature, T_g, at least detectable by DSC, suggesting their T_g could be above their thermal decomposition temperature (>500 °C). Furthermore, the DSC for a neat copolymer (curve 1) reveals transitions associated with chemical reactions, particularly one related to an endotherm between 150 and 200 °C and another one to an exotherm between 240 and 450 °C. The endotherm corresponds to the range of temperatures where BOC thermal decomposition occurs to produce PN-H,[41] as discussed in Figure 3, whereas the exotherm defines a temperature range where the cross-linking reaction by the propargyl group ($-\text{CH}_2-\text{C}\equiv\text{CH}$) may proceed.[24,29,33] The DSC analysis carried out for copolymer membranes thermally treated for 1 h at different temperatures does not present an endotherm between 150 and 200 °C (curve 2−4), confirming once again that the thermal decomposition of BOC has transformed the PN-BOC block into a PN-H block. Moreover, the DSC analysis for copolymer membranes thermally treated at 240 °C (curve 4) does really indicate that the cross-linking reaction is proceeding since there is a reduction in the area that corresponds to the exothermic cross-linking reaction. Even though it is not the goal of this research to investigate the precise cross-linking mechanisms in the whole range of temperatures, since it could be proceeding according to complex coupling reactions,[25,45] it would be interesting to prove that they are already cross-linked under some possible chemical reactions promoted under a vacuum at 240 °C for 1 h. In this regard, Figure 5 summarizes at least two possible cross-linking mechanisms, one that implies a complex coupling reaction through the triple bond in the carbon−carbon atoms (Straus coupling, Glasser coupling) to produce a linear cross-linker and another one that implies simple trimerization reactions among three acetylene end groups to form an aromatic cross-linker.[45] The solubility experiments made in NMP, and also in DMSO, carried out to determine the gel content indeed confirm that the copolymers thermally treated at 150 and 200 °C are completely soluble, indicating that the cross-linking reaction has not proceeded, whereas the copolymers that were thermally treated at 240 °C become insoluble, at 93 wt %, as compared to the initial weight immersed in NMP and DMSO, thus implicating that the propargyl cross-linking reaction has taken place. In summary, the TGA and DSC results indicate that the thermal decomposition of BOC and the cross-linking reaction can be carried out simultaneously at 240 °C for 1 h in order to produce polymeric membranes with different cross-linked chemical structures according to the mechanisms shown in Figure 5. Finally, it is important to mention that the endotherm that appears at low temperatures between 40 and 100 °C in the DSC studies could correspond, according to literature reported elsewhere,[33] to a range of temperatures where radicals are being formed. It is not the goal of this research to investigate these interesting observations.

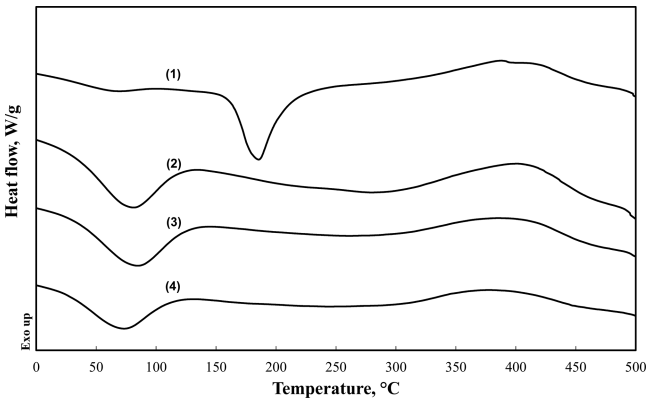

Figure 4. DSC analyses, at 10 °C/min temperature ramp under nitrogen, for $[(\text{PN-BOC})_x\text{-}(\text{PN-Pr})_y]_n$ neat copolymer membranes that were vacuum-dried at 80 °C for 24 h (1), and for neat copolymer membranes that were thermally modified, under vacuum, for 1 h at 150 °C (2), 200 °C (3), and 240 °C (4).

3.3. Gas Transport Properties. Table 1 summarizes gas permeability coefficients and ideal selectivity separation factors for several gases, at 35 °C and 2 bar, as well as the specific volume, Fractional Free Volume, FFV, and *d* spacing for $[(\text{PN-BOC})_x\text{-}(\text{PN-Pr})_y]_n$ neat copolymer membranes and for copolymer membranes thermally treated for 1 h at different temperatures. For all gases, the effect of increasing the thermal treatment temperature results in a decrease of the gas permeability coefficients with respect to the corresponding values of the neat copolymer, and this effect is associated with a densification promoted by annealing temperature and by the

DOI: 10.1021/acs.iecr.8b00529
Ind. Eng. Chem. Res. 2018, 57, 4640−4650

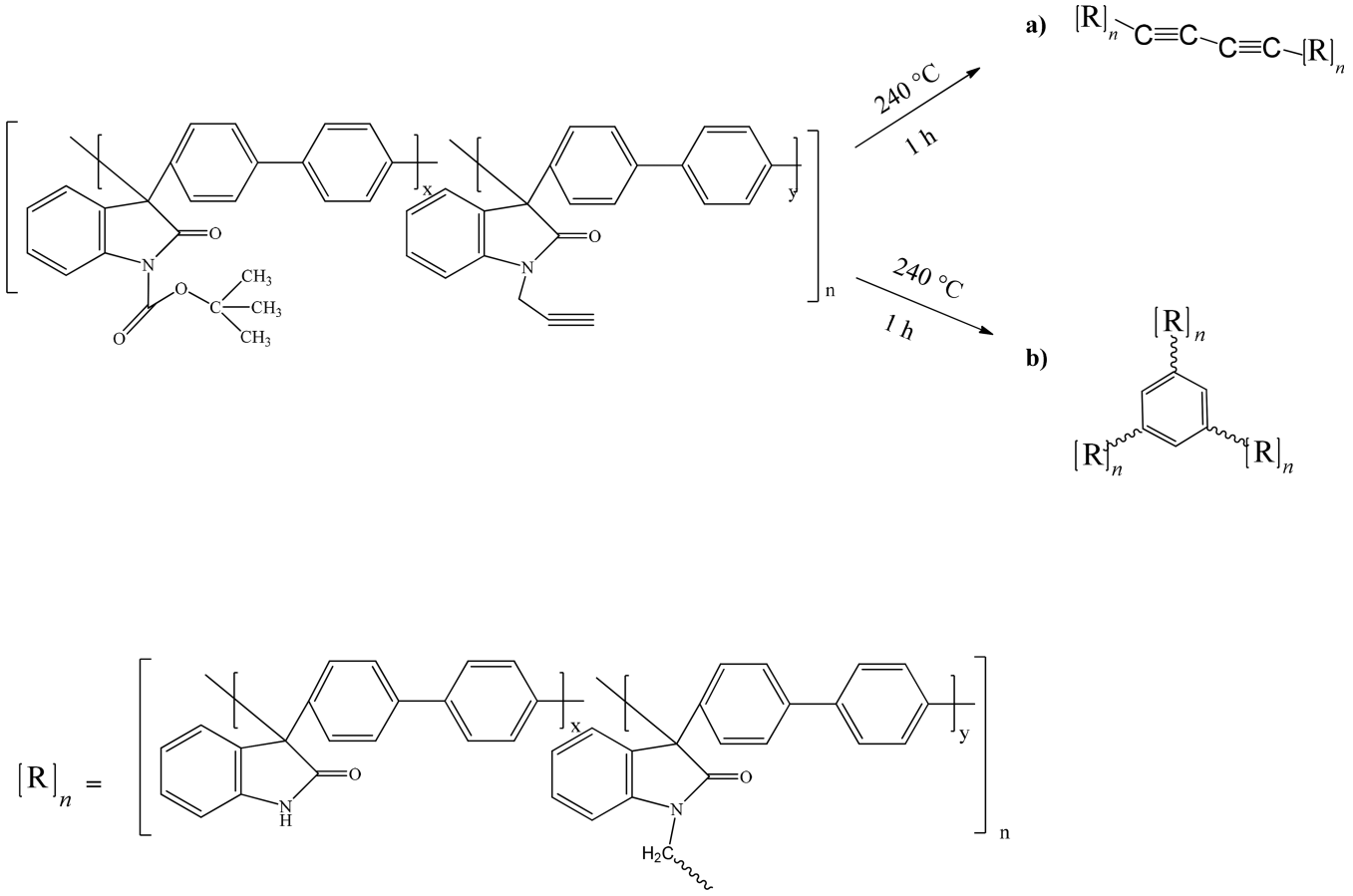

Figure 5. Possible chemical reaction mechanisms to produce a cross-linked membrane starting from a $[(\text{PN-BOC})_x\text{-}(\text{PN-Pr})_y]_n$ copolymer membrane that has been thermally treated, under vacuum, at 240 °C for 1 h. Part a implies a linear cross-linker, whereas part b implies an aromatic cross-linker.

Table 1. Gas Permeability Coefficients and Ideal Selectivity, Measured at 35 °C, 2 bar Upstream Pressure and 72 h after Thermal Treatment, as well as Specific Volume, FFV, and *d*-Spacing for Membranes Based on $[(\text{PN-BOC})_x\text{-}(\text{PN-Pr})_y]_n$ Neat Copolymer and for Membranes Thermally Treated for 1 h at Different Temperatures

	permeability coefficient,[a] $P(i)$			ideal selectivity, $P(i)/P(j)$						
thermal treatment, °C	H_2	O_2	CO_2	O_2/N_2	CO_2/N_2	H_2/CH_4	CO_2/CH_4	V(30 °C),[b] cm³/g	FFV[c]	d spacing[f] Å
neat copolymer	60	9.6	58	4.6	28	21	20	0.856	0.170	8.1; 5.4
150	58	7.6	43	5.2	29	36	27	0.829	0.147	7.6; 5.3
200	54	7.2	40	5.0	28	33	24	0.828	0.146	7.9; 5.3
240	42	5.1	32	5.4	34	40	31	0.828	0.149;[d] 0.147[e]	7.5; 5.6

[a]Permeability in Barrer (1 Barrer = 1×10^{-10} cm³ STP cm/cm² s cmHg). [b]V(30 °C) specific volume determined at 30 °C in a density gradient column. [c]FFV calculated as FFV = $[V(30\ °C) - V(0)]/V(30\ °C)$, where $V(0) = 1.3 \sum V_w$ is the occupied volume and V_w is the van der Waals volume of the repeating unit calculated from group contribution methods developed by Van Krevelen.[47] [d]FFV for a membrane made up of 93 wt % of a cross-linked membrane, assuming a linear cross-linker as depicted in Figure 5, and 7 wt % of a non-cross-linked membrane. [e]FFV for a membrane made up of 93 wt % of a cross-linked membrane, assuming an aromatic cross-linker as depicted in Figure 5, and 7 wt % of a non-cross-linked membrane. [f]Corresponding d spacing calculated from the diffraction peak maxima of amorphous polymers applying Bragg equation to WAXD scans.

chemical changes in polymer structure due to the thermal decomposition of BOC, from 150 to 200 °C, and the cross-linking reaction at 240 °C. The reductions in permeability correlate well with the corresponding reductions in specific volume, FFV, and d spacing. It is important to mention that for the evaluation of the occupied volume, $V(0)$, in the cross-linked membrane at 240 °C, it was assumed that the membrane was made up of a homogeneous blend of a 93 wt % cross-linked membrane—with at least two possible cross-linkers—and 7 wt % non-cross-linked membrane based on $[(\text{PN-H})_x\text{-}(\text{PN-Pr})_y]_n$.

In this cross-linked membrane, the net effect on the reductions in permeability, which are associated with increases in selectivity, is highly dependent on the gas kinetics diameters; i.e., the observed 46 and 44% decrease in $P(O_2)$ and $P(CO_2)$ is associated with only moderate improvements in the ideal selectivity for the gas pairs O_2/N_2, CO_2/N_2, and CO_2/CH_4; meanwhile, the 30% decrease in $P(H_2)$ is accompanied by an improvement in the H_2/CH_4 selectivity that practically duplicates the corresponding selectivity determined for the neat copolymer (increases from 21 to 40). A possible

DOI: 10.1021/acs.iecr.8b00529
Ind. Eng. Chem. Res. 2018, 57, 4640−4650

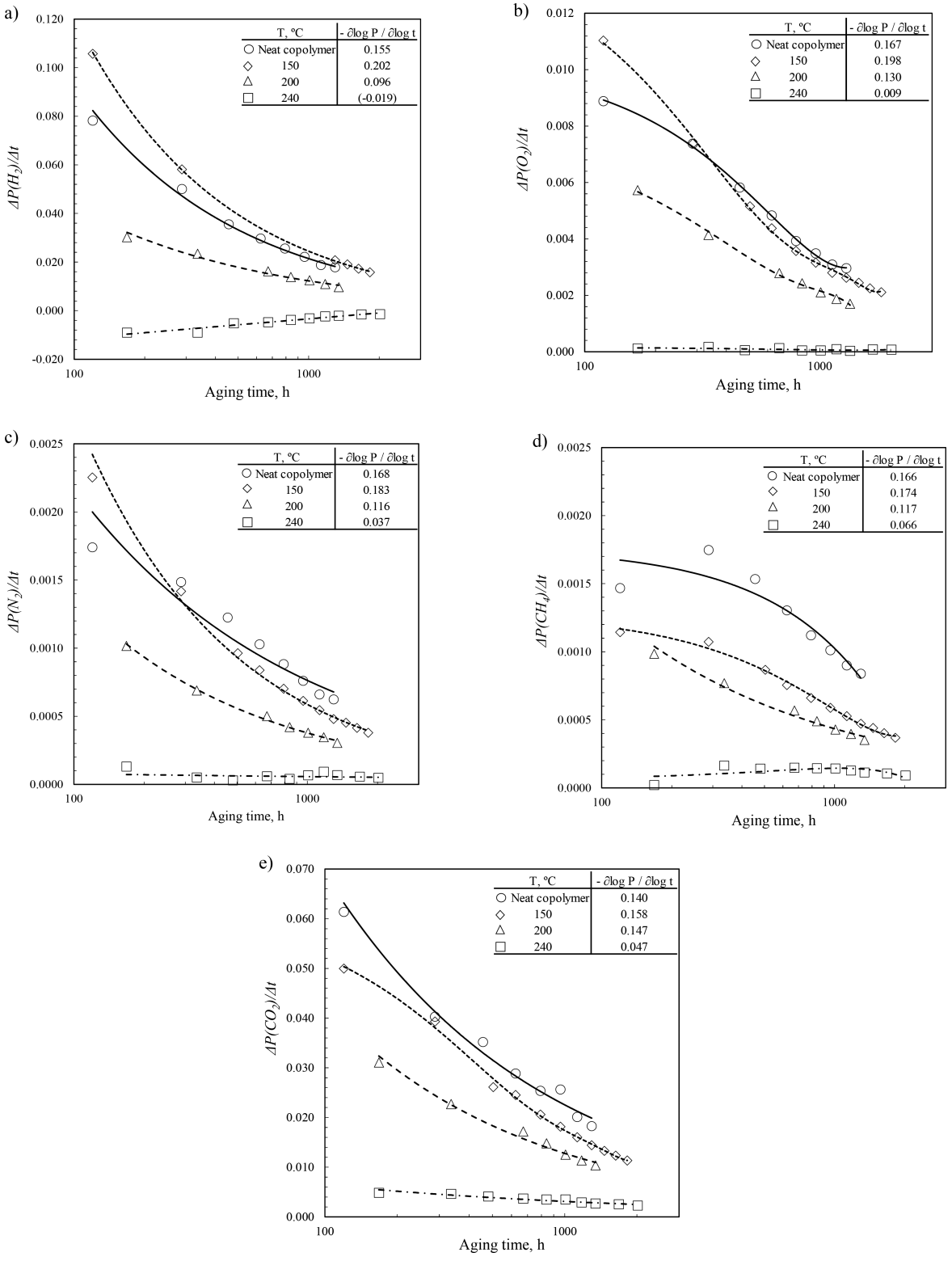

Figure 6. Permeability coefficient rates as a function of aging time calculated from H_2, O_2, N_2, CH_4, and CO_2 permeability data in membranes based on $[(\text{PN-BOC})_x\text{-}(\text{PN-Pr})_y]_n$ neat copolymer and membranes thermally treated, under vacuum, for 1 h at different temperatures. Inserted table shows the aging rate, $-\partial \log P/\partial \log t$, calculated for each gas.

explanation could be found in the fact that this membrane is made up of 93 wt % cross-linked copolymer with the remaining 7 wt % a non-cross-linked membrane. Even more, according to Figure 5, there are two possible cross-linking mechanisms, thus a 93 wt % cross-linked copolymer could be constituted of a fraction of polymer chains cross-linked by a linear cross-linker, and another fraction cross-linked with the more bulky aromatic cross-linker. Table 1 reports two FFV values that may possess the cross-linked polymer according to these two extreme mechanisms. The smaller FFV (0.147) corresponds to the case

DOI: 10.1021/acs.iecr.8b00529
Ind. Eng. Chem. Res. 2018, 57, 4640−4650

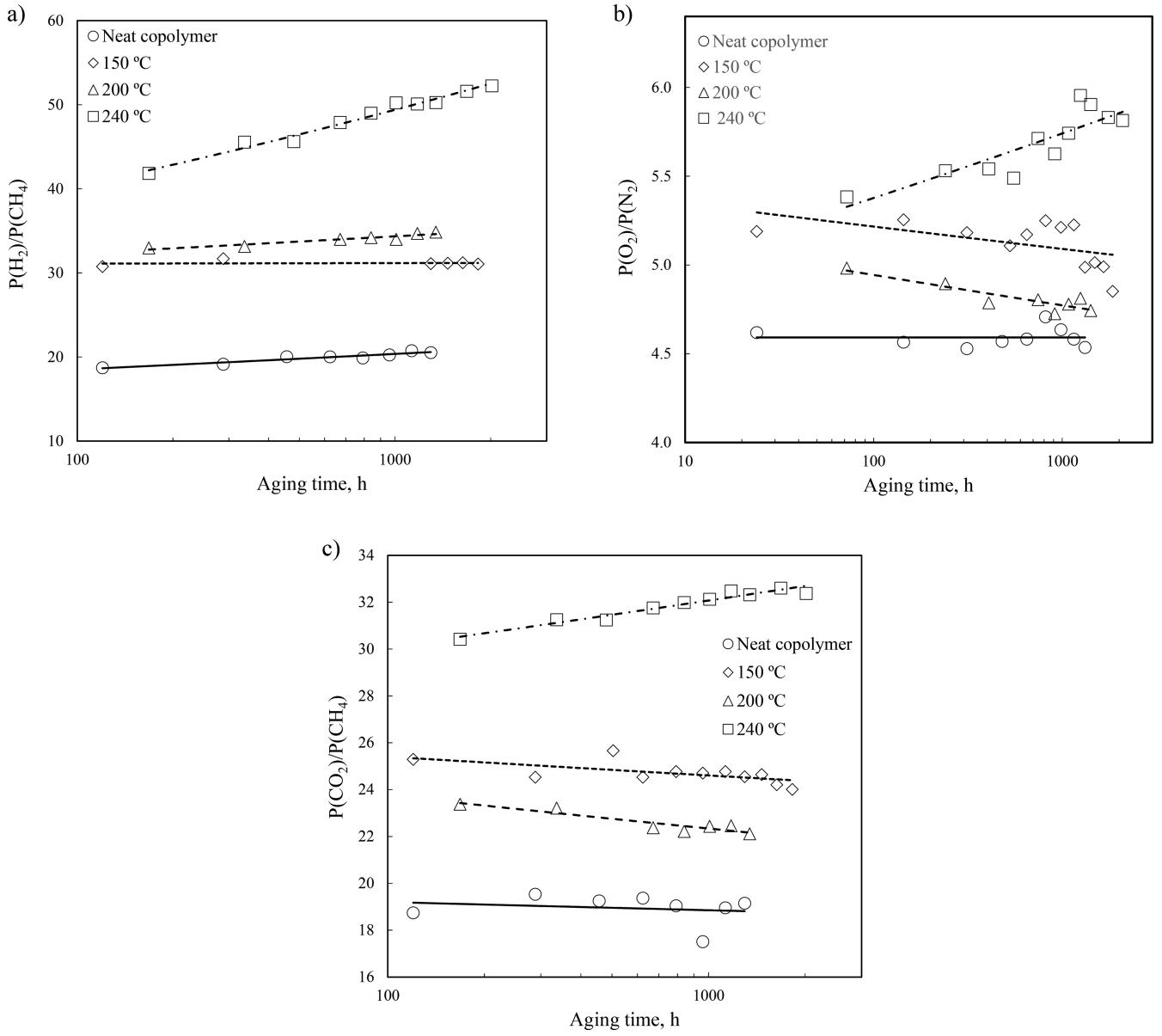

Figure 7. Ideal selectivity for the gas pairs H_2/CH_4 (a), O_2/N_2 (b), and CO_2/CH_4 (c), at 35 °C and 2 bar, as a function of aging time measured for membranes based on $[(\text{PN-BOC})_x\text{-}(\text{PN-Pr})_y]_n$ neat copolymer and membranes based on neat copolymers that were thermally treated, under a vacuum, for 1 h at different temperatures.

where all repeating units are cross-linked by a linear cross-linker. The larger FFV (0.149) corresponds to the assumption where the bulky aromatic cross-linker leads to a cross-linked copolymer membrane.

Figure 6 shows the H_2, O_2, N_2, CH_4, and CO_2 gas permeability coefficient change as a function of aging time, $\Delta P(i)/\Delta t$, measured at 35 °C and 2 bar, in $[(\text{PN-BOC})_x\text{-}(\text{PN-Pr})_y]_n$ neat copolymer and membranes thermally treated for 1 h at different temperatures. The inset in Figure 6 reports the aging rate, $[-\partial \log P/\partial \log t]$, as it is typically defined elsewhere.[12,16] For every gas, the permeability coefficient change, as it is defined in this work, is noticeable higher in both the neat copolymer and the membranes thermally treated at 150 and 200 °C than the corresponding change in the cross-linked membrane at 240 °C. Similarly, the aging rate (inserted in the table of Figure 6) is being decreased as the chemical changes in the polymer repeating units are occurring with temperature until they are relatively small for the case of the cross-linked membrane. Cross-linking has already mitigated the effect of aging time in the permeability coefficients, and this may be a consequence of a decrease in the relaxed free volume, RFV, which at any temperature below the glass transition temperature is defined by the difference between the specific volume at the glassy state (a nonequilibrium state), $V_g(T)$, minus the specific volume in the crystalline state (equilibrium state), $V_c(T)$. In other words, as the RFV approaches zero, it will present less change in densification with aging time. This fundamental explanation, based on the typical specific volume−temperature behavior in glassy polymers, is indirectly proved by the experimental decreases in the aging rates with thermal treatment temperature. Since the aging rate for each gas in the cross-linked membrane is not still zero and depends on the type of gas being permeated, it is interesting to analyze the effect of aging time, under a high vacuum (10^{-3} Torr), on the associated changes in permeability. It stands, for the gases with large kinetics diameters, in the order $CH_4 > N_2 > CO_2 > O_2$. The

DOI: 10.1021/acs.iecr.8b00529
Ind. Eng. Chem. Res. 2018, 57, 4640−4650

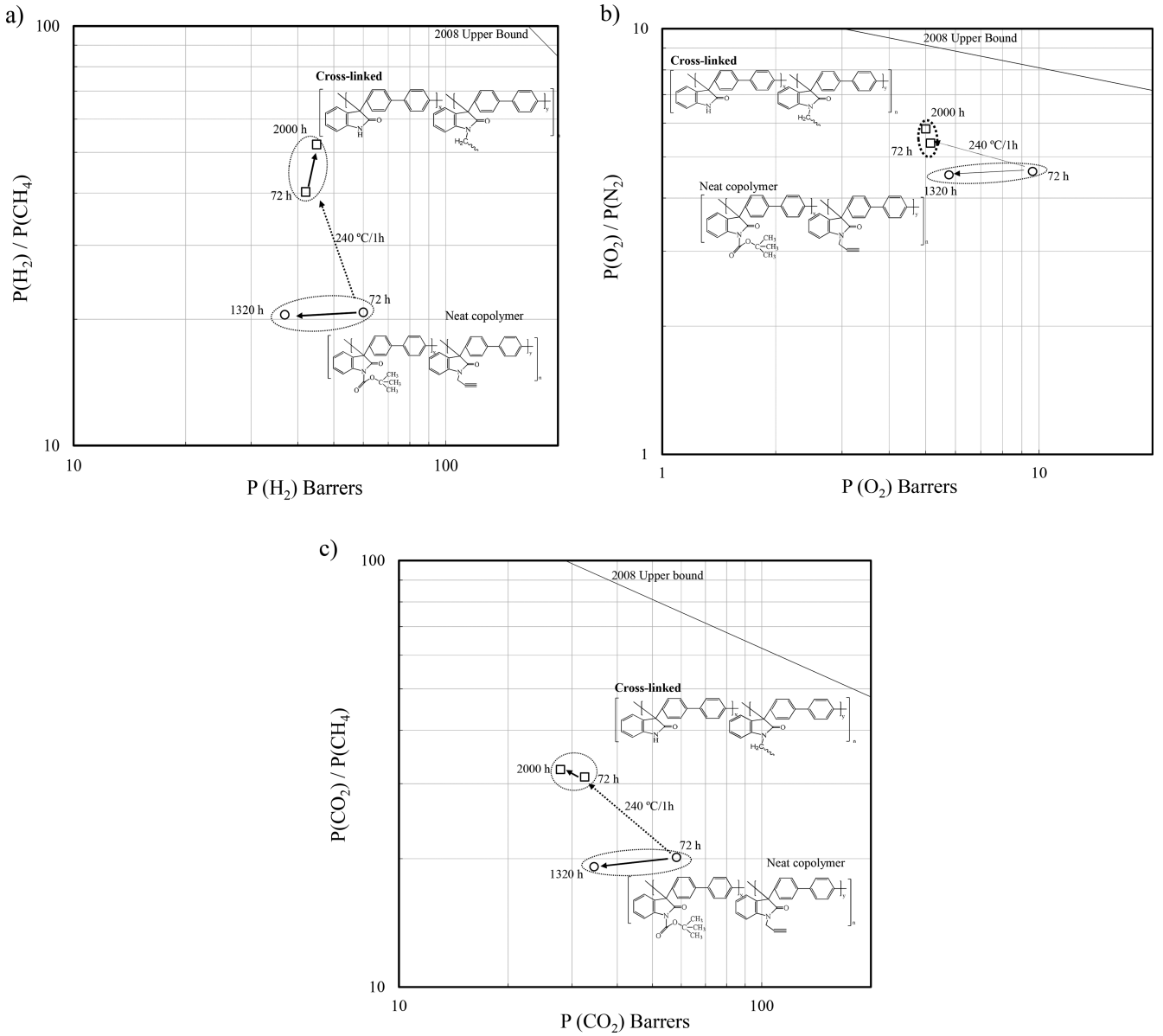

Figure 8. Effect of annealing, under a high vacuum (10^{-3} Torr), on the ideal selectivity−permeability relationship for the gas pairs H_2/CH_4 (a), O_2/N_2 (b), and CO_2/CH_4 (c), at 35 °C and 2 bar, determined for membranes based on $[(PN\text{-}BOC)_x\text{-}(PN\text{-}Pr)_y]_n$ neat copolymer and membranes based on neat copolymers that were thermally treated, under a vacuum, for 1 h at different temperatures. Robeson's 2008 upper bound[46] is shown as a reference line.

effect of vacuum-aging is more notorious in the permeability values of CH_4, N_2, and CO_2, and less for the case of O_2, which reports an aging rate of 0.009. Particularly for H_2, the aging rate is positive, meaning that $P(H_2)$ is slightly increasing with aging time. Of course, these changes have to be reflected in the gas selectivity of the membranes depending on the type of gas pair to be considered.

Figure 7 shows the corresponding ideal separation factors as a function of aging time for the gas pairs H_2/CH_4, O_2/N_2, and CO_2/CH_4. For any gas pair shown, the selectivity in any membrane, cross-linked or non-cross-linked, does not change drastically with aging time, just as would be expected. However, specifically for the gas pair H_2/CH_4, selectivity increases from 40 to 50, which confirms that the densification process is still ongoing, even though it has been mitigated by cross-linking. Moreover, the fact that selectivity increases with aging time under a high vacuum suggests that the change in the relaxed free volume in the cross-linked membrane leads to free volume redistributions from "big transient holes" to "small transient holes." These redistributions should be favorable to gases with small kinetics diameters such as H_2, which is experimentally supported from a positive aging rate, and unfavorable to large kinetics diameters, as is experimentally represented for a negative aging rate that stands in the order $CH_4 > N_2 > CO_2 > O_2$. Perhaps a polymer subjected to aging under a high vacuum (10^{-3} Torr), as is the case for the 12 to 20 μm films studied in this work, leads to different free volume redistributions as compared to the corresponding redistributions as it was being aged at atmospheric temperature and pressure.

Figure 8 shows the selectivity−permeability combination of properties for the gas pairs H_2/CH_4, O_2/N_2, and CO_2/CH_4, at 35 °C and 2 bar, for $[(PN\text{-}BOC)_x\text{-}(PN\text{-}Pr)_y]_n$ neat copolymer and the cross-linked membranes. In order to evaluate the effect of aging time on the gas selectivity−permeability combination

DOI: 10.1021/acs.iecr.8b00529
Ind. Eng. Chem. Res. 2018, 57, 4640−4650

of properties, only the corresponding values determined at 72 h and the longest aging time (~2000 h) have been included. For the neat copolymer and for the three gas pairs, as aging time increases, its gas permeability coefficients decrease without changing its ideal selectivity factor. If the neat copolymer is thermally treated for 1 h at 240 °C to simultaneously decompose the thermolabile BOC group and to cross-link the repeating units through the propargyl group, the resulting cross-linked membrane possesses a higher ideal selectivity factor with the increase being at the expense of a decrease in the permeability coefficient of the fastest gas; in other words, the typical trade-off is still observed. However, in regard to the effect of aging time under a high vacuum, for the gas pairs O_2/N_2 and CO_2/CH_4, the selectivity−permeability relationship in the cross-linked membrane remains with slight variations with aging time, of course, as compared to the corresponding relationship for the non-cross-linked or neat copolymer membrane; meanwhile, the selectivity−permeability relationship for H_2/CH_4 moves in the direction of improved permeability and improved selectivity. As mentioned, the effect of aging time in the $P(H_2)$ aging rate is slightly positive, $[-\partial \log P/\partial \log t] = -0.019$, whereas the effect on $P(CH_4)$ is high and negative, $[-\partial \log P/\partial \log t] = 0.066$.

4. CONCLUSIONS

A copolymer based on a poly(oxyindole biphenylylene) bearing both a thermolabile BOC group and a propargyl unsaturated group, $[(\text{PN-BOC})_x\text{-}(\text{PN-Pr})_y]_n$, has been successfully synthesized at room temperature starting from a poly(oxyindole biphenylylene) bearing just a H atom (PN-H). DSC results show that the copolymers synthesized in this work do not present a detectable T_g. TGA studies reveal that the copolymers are highly stable at elevated temperatures since their main chain decomposition temperatures are higher than 500 °C. TGA and DSC studies reveal that it is possible to follow the BOC decomposition kinetics and the cross-linking reaction at 240 °C to produce a copolymer membrane made up of a 93 wt % cross-linked copolymer and 7 wt % non-cross-linked copolymer. With the copolymers synthesized and analyzed through systematic studies on structure/processing/property relationships assessed by TGA, DSC, and permeability, it is demonstrated that the simultaneous decomposition of BOC and cross-linking of the copolymer chains at 240 °C for 1 h leads to cross-linked membranes that are chemically robust (insoluble in NMP and DMSO) and physically resistant to aging since the reduction in the gas permeability coefficients with time, and the aging rates, are approaching zero, at least during the 2000 h of the measurements performed in membranes with thicknesses between 12 and 20 μm, and that were subjected to a high vacuum (10^{-3} Torr) during the aging study. As a consequence, the densification rate in these types of copolymers has been mitigated.

AUTHOR INFORMATION

Corresponding Author

*Phone: +52(55)5950-4000 x 4732. E-mail alberto.ruiz@ibero.mx.

ORCID

F. Alberto Ruiz-Treviño: 0000-0002-6476-8137
Manuel J. Aguilar-Vega: 0000-0002-8473-3628
Mikhail G. Zolotukhin: 0000-0001-7395-7354
Lilian I. Olvera: 0000-0002-1505-2319

Notes

The authors declare no competing financial interest.

ACKNOWLEDGMENTS

The authors acknowledge financial support from CONACYT Grants CB-2012-01-184156 and 251693 and DGAPA-UNAM (PAPIIT and IN 203517). Hugo Hernández-Martínez thanks CONACYT and Universidad Iberoamericana for the scholarship. Thanks are due to E. R. Morales and S. Morales for assistance with thermal and spectroscopic analysis. The authors also thank A. Lopez Vivas and Alejandro Pompa for technical help.

REFERENCES

(1) Powell, C.; Qiao, C. Polymeric CO_2/N_2 gas separation membranes for the capture of carbon dioxide from power plant flue gas. *J. Membr. Sci.* **2006**, *279*, 1−49.
(2) Mannan, H. A.; Mukhtar, H.; Murugesan, T.; Nasir, R.; Mohshim, D. F.; Mushtaq, A. Recent applications of polymer blends in gas separation membranes. *Chem. Eng. Technol.* **2013**, *36*, 1838.
(3) Yampolskii, Y. Polymeric gas separation membranes. *Macromolecules* **2012**, *45*, 3298−3311.
(4) He, X.; Hägg, M. B. Membranes for environmentally friendly energy processes. *Membranes* **2012**, *2* (4), 706−726.
(5) Xu, L.; Rungta, M.; Hessler, J.; Qiu, W.; Brayden, M.; Martínez, M.; Barbay, G.; Koros, W. J. Physical aging in carbon molecular sieve membranes. *Carbon* **2014**, *80*, 155−166.
(6) Swaidan, R.; Ghanem, B.; Litwiller, E.; Pinnau, I. Physical aging, plasticization and their effects on gas permeation in "Rigid" polymers of intrinsic microporosity. *Macromolecules* **2015**, *48* (18), 6553−6561.
(7) Zhang, C.; Li, P.; Cao, B. Decarboxylation crosslinking of polyimides whit high CO_2/CH_4 separation performance and plasticization resistance. *J. Membr. Sci.* **2017**, *528*, 206−216.
(8) Zhang, C.; Cao, B.; Li, P. Thermal oxidative crosslinking of phenolphthalein-based cardo polyimides with enhanced gas permeability and selectivity. *J. Membr. Sci.* **2018**, *546*, 90−99.
(9) Strum, L. C. E. Physical aging in plastics and other glassy materials. *Polym. Eng. Sci.* **1977**, *17*, 165−173.
(10) Hutchinson, J. M. Physical aging of polymers. *Prog. Polym. Sci.* **1995**, *20*, 703−760.
(11) Baker, R. W.; Low, B. T. Gas separation membrane materials: A perspective. *Macromolecules* **2014**, *47*, 6999−7013.
(12) Tiwari, R. R.; Smith, Z. P.; Lin, H.; Freeman, B. D.; Paul, D. R. Gas permeation in thin films of "high free-volume" glassy perfluoropolymers: Part I. Physical aging. *Polymer* **2014**, *55*, 5788−5800.
(13) Ho, C. H.; Vu-Khanh, T. Effects of time and temperature on physical aging of polycarbonate. *Theor. Appl. Fract. Mech.* **2003**, *39*, 107−116.
(14) Huang, Y.; Paul, D. R. Effect of temperature on physical aging of thin glassy polymer films. *Macromolecules* **2005**, *38*, 10148−10154.
(15) Rowe, B. W.; Freeman, B. D.; Paul, D. R. Influence of previous history on physical aging in thin glassy polymer films as gas separation membranes. *Polymer* **2010**, *51*, 3784−3792.
(16) Murphy, T. M.; Langhe, D. S.; Ponting, M.; Baer, E.; Freeman, B. D.; Paul, D. R. Physical aging of layered glassy polymer films via gas permeability tracking. *Polymer* **2011**, *52*, 6117−6125.
(17) Rezac, M. E.; Sorensen, E. T.; Beckham, H. W. Transport properties of crosslinkable polyimide blends. *J. Membr. Sci.* **1997**, *136*, 249−259.
(18) Huang, Y.; Wang, X.; Paul, D. R. Physical aging of thin glassy polymer films: Free volume interpretation. *J. Membr. Sci.* **2006**, *277*, 219−229.
(19) Wang, H.; Chung, T. S.; Paul, D. R. Physical aging and plasticization of thick and thin films of the thermally rearranged ortho-functional polyimide 6FDA-HAB. *J. Membr. Sci.* **2014**, *458*, 27−35.

DOI: 10.1021/acs.iecr.8b00529
Ind. Eng. Chem. Res. 2018, 57, 4640−4650

(20) Ansaloni, L.; Minelli, M.; Giacinti Baschetti, M.; Sarti, G. C. Effects of thermal treatment and physical aging on the gas transport properties in Matrimid®. *Oil Gas Sci. Technol.* **2015**, *70* (2), 367−379.
(21) Yavari, M.; Maruf, S.; Ding, Y.; Lin, H. Physical aging of glassy perfluropolymers in thin film composite membranes. Part II. Glass transition temperature and the free volume model. *J. Membr. Sci.* **2017**, *525*, 399−408.
(22) Kim, J. H.; Koros, W. J.; Paul, D. R. Effects of CO_2 exposure and physical aging on the gas permeability on thin 6FDA polyimide membranes Part 1. Without crosslinking. *J. Membr. Sci.* **2006**, *282*, 21−31.
(23) Kim, J. H.; Koros, W. J.; Paul, D. R. Effects of CO_2 exposure and physical aging on the gas permeability on thin 6FDA polyimide membranes Part 2. With crosslinking. *J. Membr. Sci.* **2006**, *282*, 32−43.
(24) Lee, K. S.; Jeong, M. H.; Lee, J. P.; Lee, J. S. End-group cross-linked poly (arylene ether) for proton exchange membranes. *Macromolecules* **2009**, *42* (3), 584−590.
(25) Chul Gil, S.; Chul Kim, J.; Ahn, D.; Jang, J. S.; Kim, H.; Chul Jung, J.; Lim, S.; Jung, D. H.; Lee, W. Thermally crosslinked sulfonated polyethersulfone proton exchange membranes for direct methanol fuel cells. *J. Membr. Sci.* **2012**, *417*, 2−9.
(26) Iqbal, M.; Norder, B.; Mendes, E.; Dingemans, T. J. All-aromatic liquid crystalline thermosets with high glass transition temperatures. *J. Polym. Sci., Part A: Polym. Chem.* **2009**, *47* (5), 1368−1380.
(27) Choi, J. H.; Choi, K. M.; Jeon, H. J.; Choi, Y. J.; Lee, Y.; Kang, J. K. Acetylene gas mediated conjugated microporous polymers (ACMPs): first use of acetylene gas as a building unit. *Macromolecules* **2010**, *43* (13), 5508−5511.
(28) Agag, T.; Takeichi, T. Novel benzoxazine monomers containing p-phenyl propargyl ether: polymerization of monomers and properties of polybenzoxazines. *Macromolecules* **2001**, *34* (21), 7257−7263.
(29) Dogan-Demir, K.; Kiskan, B.; Yagci, Y. Thermally curable acetylene-containing main-chain benzoxazine polymers via sonogashira coupling reaction. *Macromolecules* **2011**, *44* (7), 1801−1807.
(30) Gao, Y.; Huang, F.; Zhou, Y.; Du, L. Synthesis and characterization of a novel acetylene and maleimide terminated benzoxazine and its high-performance thermosets. *J. Appl. Polym. Sci.* **2013**, *128* (1), 340−346.
(31) Luo, Y.; Sun, J.; Jin, K.; Wang, J.; Huang, G.; Fang, Q. Propargyl ether-functionalized poly (m-phenylene): a new precursor for the preparation of polymers with high modulus and high Tg. *RSC Adv.* **2015**, *5* (29), 23009−23014.
(32) Zhou, J.; Wang, J.; Jin, K.; Sun, J.; Fang, Q. s-Triazine-based functional monomers with thermocrosslinkable propargyl units: Synthesis and conversion to the heat-resistant polymers. *Polymer* **2016**, *102*, 301−307.
(33) Secker, C.; Brosnan, S. M.; Limberg, F. R.; Braun, U.; Trunk, M.; Strauch, P.; Schlaad, H. Thermally induced crosslinking of poly (N-propargyl glycine). *Macromol. Chem. Phys.* **2015**, *216* (21), 2080−2085.
(34) Zhou, X.; Obadia, M. M.; Venna, S. R.; Roth, E. A.; Serghei, A.; Luebke, D. R.; Myers, C.; Chang, Z.; Enick, R.; Drockenmuller, E.; Nulwala, H. B. Highly cross-linked polyether-based 1, 2, 3-triazolium ion conducting membranes with enhanced gas separation properties. *Eur. Polym. J.* **2016**, *84*, 65−76.
(35) Park, H. B.; Jung, C. H.; Lee, Y. M.; Hill, A. J.; Pas, S. J.; Mudie, S. T.; Van Wagner, E.; Freeman, B. D.; Cookson, D. J. Polymers with cavities tuned for fast selective transport of small molecules and ions. *Science* **2007**, *318*, 254−258.
(36) Thornton, A. W.; Nairn, K. M.; Hill, A. J.; Hill, J. M. New relation between diffusion and free volume: predicting gas diffusion. *J. Membr. Sci.* **2009**, *338*, 29−37.
(37) Park, H. B.; Han, S. H.; Jung, C. H.; Lee, Y. M.; Hill, A. J. Thermally rearranged (TR) polymer membranes for CO_2 separation. *J. Membr. Sci.* **2010**, *359*, 11−24.
(38) Sanders, D. F.; Smith, Z. P.; Ribeiro, C. P., Jr.; Guo, R.; McGrath, J. E.; Paul, D. R.; Freeman, B. D. Gas permeability, diffusivity, and free volume of thermally rearranged polymers based on 3,3′-dihydroxy-4,4′-diamino-biphenyl (HAB) and 2,2′-bis-(3,4-dicarboxyphenyl) hexafluoropropane dianhydride (6FDA). *J. Membr. Sci.* **2012**, *409−410*, 232−241.
(39) Merlet, S.; Marestin, C.; Schiets, F.; Romeyer, O.; Mercier, R. Preparation and characterization of nanocellular poly-(phenylquinoxaline) foams. A new approach to nanoporous high-performance polymers. *Macromolecules* **2007**, *40* (6), 2070−2078.
(40) Xiao, Y.; Chung, T. S. Grafting thermally labile molecules on cross-linkable polyimide to design membrane materials for natural gas purification and CO_2 capture. *Energy Environ. Sci.* **2011**, *4*, 201−208.
(41) Sanchez-Garcia, S.; Ruiz-Treviño, F. A.; Aguilar-Vega, M. J.; Zolotukhin, M. G. Gas permeability and selectivity in thermally modified poly(oxyindole biphenylylene) membranes bearing a tert-butyl carbonate group. *Ind. Eng. Chem. Res.* **2016**, *55*, 7012−7020.
(42) Hernandez, M. C. G.; Zolotukhin, M. G.; Fomine, S.; Cedillo, G.; Morales, S. L.; Frohlich, N.; Preis, E.; Scherf, U.; Salmon, M.; Chavez, M. I.; Cardenas, J.; Ruiz-Trevino, A. Novel, metal-free, superacid-catalyzed "click" reactions of isatins with linear, non-activated, multiring aromatic hydrocarbons. *Macromolecules* **2010**, *43*, 6968−6979.
(43) Cruz, A. R.; Hernández, M. C. G.; Guzman-Gutierrez, M. T.; Zolotukhin, M. G.; Fomine, S.; Morales, S. L.; Kricheldorf, H.; Wilks, E. S.; Cárdenas, J.; Salmon, M. Precision synthesis of narrow polydispersity ultrahigh molecular weight linear aromatic polymers by A2 + B2 nonstoichiometric step-selective polymerization. *Macromolecules* **2012**, *45*, 6774−6780.
(44) Camacho-Zuñiga, C.; Ruiz-Treviño, F. A.; Zolotukhin, M. G.; Del Castillo, L. F.; Guzmán, J.; et al. Gas transport properties of new aromatic cardo poly(aryl ether ketone)s. *J. Membr. Sci.* **2006**, *283*, 393−398.
(45) Kovar, R. F.; Ehlers, G. F. L.; Arnold, F. E. Thermosetting acetylene-terminated polyphenylquinoxalines. *J. Polym. Sci., Polym. Chem. Ed.* **1977**, *15*, 1081−1095.
(46) Robeson, L. M. The upper bound revisited. *J. Membr. Sci.* **2008**, *320*, 390−400.
(47) Van Krevelen, D. W. *Properties of Polymers: Their Correlation with Chemical Structure, Their Numerical Estimation and Prediction from Additive Group Contributions*; Elsevier: Amsterdam, The Netherlands, 1960.

DOI: 10.1021/acs.iecr.8b00529
Ind. Eng. Chem. Res. 2018, 57, 4640−4650